Hindawi Publishing Corporation
Mathematical Problems in Engineering
Volume 2013, Article ID 915781, 8 pages
http://dx.doi.org/10.1155/2013/915781

Research Article

Numerical Study of Surface Roughness and Magnetic Field between Rough and Porous Rectangular Plates

Ramesh B. Kudenatti,[1] Shalini M. Patil,[2] P. A. Dinesh,[3] and C. V. Vinay[2]

[1] *Department of Mathematics, Bangalore University, Bangalore 560001, India*
[2] *Department of Mathematics, JSSATE, Bangalore 560060, India*
[3] *Department of Mathematics, MSRIT, Bangalore 560054, India*

Correspondence should be addressed to Shalini M. Patil; shahem_blr@yahoo.co.in

Received 25 July 2013; Revised 30 October 2013; Accepted 31 October 2013

Academic Editor: Jun Jiang

This paper theoretically examines the combined effects of surface roughness and magnetic field between two rectangular parallel plates of which the upper plate has roughness structure and the lower plate has porous material in the presence of transverse magnetic field. The lubricating fluid in the film region is assumed to be Newtonian fluid (linearly viscous and incompressible fluid). This model consists of mathematical formulation of the problem with appropriate boundary conditions and solution numerically by finite difference based multigrid method. The generalized average modified Reynolds equation is derived for longitudinal roughness using Christensen's stochastic theory which assumes that the height of the roughness asperity is of the same order as the mean separation between the plates. We obtain the bearing characteristics such as pressure distribution and load carrying capacity for various values of roughness, Hartmann number, and permeability parameters. It is observed that the pressure distribution and load carrying capacity were found to be more pronounced for increasing values of roughness parameter and Hartmann number; whereas these are found to be decreasing for increasing permeability compared to their corresponding classical cases. The physical reasons for these characters are discussed in detail.

1. Introduction

It is unrealistic that there exists a perfectly smooth surface. Since all the surfaces are rough to some extent, the surface roughness percentage (degree) may vary from polished surfaces to machined surfaces. Rough surfaces usually wear more quickly and have higher frictional coefficients than smooth surfaces. The interesting observation is that the bearing geometry and roughness type affect the measure of influence of surface roughness. It is a piece of evidence that surface roughness of the bearings considerably affect its performance. Bearing surfaces develop roughness after having some run in and wear. On the other hand, other reason to generate roughness is contamination of the lubricant. In view of this, many scientists and mathematicians proposed to study the effect of surface roughness on bearing surfaces (a saw tooth curve model by Davies [1], the Fourier series type approximation by Burton [2], and so on). Since the surface roughness distribution is random in nature, a stochastic approach has to be adopted. A stochastic theory for the study of rough surfaces in hydrodynamic lubrication was investigated by Christensen [3]. Since then many researchers have adopted and used extensively this approach to study roughness effect on bearing surfaces, narrow journal bearings by Gururajan and Prakash [4], finite journal bearings by Chiang et al. [5], poroelastic bearings by Bujurke and Kudenatti [6], and so on.

MHD is the physical-mathematical framework that concerns the dynamics of magnetic field in electrically conducting fluids. The presence of magnetic field leads to the forces that in turn act on the fluid, thereby potentially altering the geometry (topology). Some of the other phenomena of various fields like science, astrophysics, geophysics, engineering, and technology involve MHD. The applications of MHD are MHD generators, MHD pumps, fusion reactors, crystal growth, magnetic drug targeting, and metallurgical applications. Theoretically and experimentally several investigations

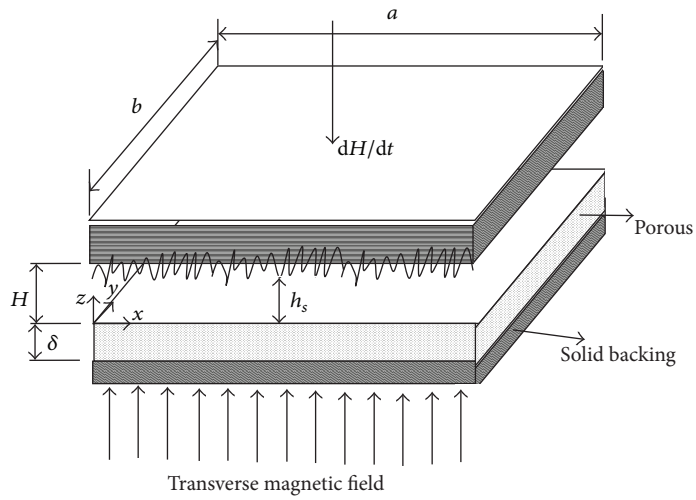

Figure 1: The physical configuration of squeeze film between rough and porous rectangular plate in the presence of magnetic field.

have taken place on MHD lubrication. Many theoretical studies on MHD lubrication are available in the literature which includes MHD slider bearings (MHD Journal bearings Kamiyama [7], Anwar and Rodkiewicz [8], effects of MHD by Hamza [9], Maki et al. [10], and Shukla [11]). Recently, Bujurke and Kudenatti [12] have theoretically explored the effect of roughness on the electrically conducting fluid in the rectangular plates, in which upper plate has a rough structure, and found that the effect of roughness and Hartmann number is to increase the pressure distribution and hence the load carrying capacity for increasing roughness and magnetic parameters.

We investigate the combined effects of surface roughness and magnetic field on squeeze film lubrication characteristics between two plates of which an upper plate has a roughness structure and the lower plate has a porous material in the presence of uniform applied transverse magnetic field.

This paper is organized into the following different sections. The basic governing equations with supporting boundary conditions are given and consequently modified MHD Reynolds equation is derived in Section 2. The Reynolds equation for longitudinal roughness is derived in this section to study the effect of roughness. Finite difference based multigrid method is adopted to obtain the pressure distribution and load carrying capacity in Section 3. In Section 4, we analyse bearing characteristics for varying roughness parameters, Hartmann number, aspect ratio, and permeability. Important findings and their significances are summarized in the final section.

2. Formulation of the Problem

This model consists of flow of viscous isothermal and incompressible (Newtonian) electrically conducting fluid between two rectangular plates in which the upper plate has a rough structure. The physical configuration of the problem is shown in Figure 1. The upper rough plate approaches the lower smooth plate with a constant velocity dH/dt. A uniform transverse magnetic field M_0 is applied in the z-direction. The upper and lower plates are separated by thickness H, then, the total film thickness is made up of two parts as

$$H = h_0 + h_s(x, y, \xi), \tag{1}$$

where h_0 is the height of the nominal smooth part of the film region, h_s is part due to the surface asperities measured from the nominal level which is a randomly varying quantity of zero mean, and ξ is the index parameter determining a definite roughness structure.

In addition to the usual assumptions of lubrication theory, we assume fluid inertia to be negligible and, except the Lorentz force, the body forces are also neglected. Under these assumptions, the governing equations in Cartesian coordinates system are

$$\frac{\partial u}{\partial x} + \frac{\partial v}{\partial y} + \frac{\partial w}{\partial z} = 0, \tag{2}$$

$$\frac{\partial p}{\partial x} = \mu \frac{\partial^2 u}{\partial z^2} - \sigma M_0^2 u, \tag{3}$$

$$\frac{\partial p}{\partial y} = \mu \frac{\partial^2 v}{\partial z^2} - \sigma M_0^2 v, \tag{4}$$

$$\frac{\partial p}{\partial z} = 0, \tag{5}$$

where u, v, and w are the velocity components in x, y, and z directions, respectively, p is the pressure, σ is electrical conductivity of the fluid, M_0 is the impressed magnetic field, and μ is viscosity of the fluid. The relevant boundary conditions for the velocity components are mentioned below.

At the upper solid rough surface $z = H$ one has

$$u = 0, \qquad v = 0, \qquad w = \frac{\partial H}{\partial t}, \tag{6}$$

and at the lower porous surface at $z = 0$ one has

$$\frac{\alpha}{\sqrt{k}}\left(u - u^*\right) = \frac{\partial u}{\partial z}, \tag{7}$$

$$\frac{\alpha}{\sqrt{k}}\left(v - v^*\right) = \frac{\partial v}{\partial z}, \tag{8}$$

$$w = w^*. \tag{9}$$

The slip velocity boundary conditions (7) and (8) are due to the Beavers and Joseph [13] slip conditions, where α is the dimensionless slip constant that depends on the characteristics of the porous medium and k is the permeability parameter.

The modified form of the Darcy law, which governs the flow of a Newtonian fluid and applied magnetic field in the porous region, is given by

$$u^* = \frac{-k}{\mu\left(1 + \varphi M^2\right)}\frac{\partial P^*}{\partial x}, \tag{10a}$$

$$v^* = \frac{-k}{\mu\left(1 + \phi M^2\right)}\frac{\partial P^*}{\partial y}, \tag{10b}$$

$$w^* = \frac{-k}{\mu}\frac{\partial P^*}{\partial z}, \tag{10c}$$

$$\nabla \cdot \mathbf{q}^* = 0, \tag{11}$$

where $\mathbf{q}^* = (u^*, v^*, w^*)$ are velocity components in x, y, and z directions, φ is the porosity parameter, M $(= M_0\sqrt{(\sigma/\mu)}h_0)$ denotes the nondimensional magnetic (Hartmann) number and gives the effect of magnetic field on squeeze film lubrication and $\mathbf{P}^*$ is the hydrostatic pressure. It readily follows from (10a), (10b), (10c), and (11) that the pressure $\mathbf{P}^*$ in the porous region obeys the Laplace equation

$$\frac{\partial^2 P^*}{\partial x^2} + \frac{\partial^2 P^*}{\partial y^2} + D\frac{\partial^2 P^*}{\partial z^2} = 0, \tag{12}$$

where $D = (1 + \phi M^2)$.

Integrating the Laplace equation (12) with respect to z from $-\delta$ to 0 using the solid backing boundary condition $\partial P^*/\partial z = 0$ at $z = -\delta$, we get

$$\left.\frac{\partial P^*}{\partial z}\right|_{z=0} = -\frac{1}{D}\int_{-\delta}^{0}\left(\frac{\partial^2 p}{\partial x^2} + \frac{\partial^2 p}{\partial y^2}\right)dz, \tag{13}$$

where δ is the thickness of the porous region. Using Morgan and Cameron [14] approximation which assumes that the thickness of porous region is too small compared to the fluid film region, and then using interface boundary condition $p = P^*$ at $z = 0$, (13) becomes

$$\left.\frac{\partial P^*}{\partial z}\right|_{z=0} = -\frac{\delta}{D}\left(\frac{\partial^2 p}{\partial x^2} + \frac{\partial^2 p}{\partial y^2}\right). \tag{14}$$

Plugging the solutions of (3) and (4) for u and v into the continuity equation (2) and integrating it with respect to z across the fluid film thickness using boundary conditions (6) and (9), we get the following modified Reynolds equation describing pressure distribution in the fluid film region:

$$\frac{\partial}{\partial x}\left\{F(H, M)\frac{\partial p}{\partial x}\right\} + \frac{\partial}{\partial y}\left\{F(H, M)\frac{\partial p}{\partial y}\right\} = -\left(\frac{\partial H}{\partial t} + \frac{k}{\mu}\left.\frac{\partial P^*}{\partial z}\right|_{z=0}\right), \tag{15}$$

where

$$\begin{aligned} F(H, M) &= \left(A_1\left(\cosh\left(\frac{MH}{h_0}\right) - 1\right)\right. \\ &\quad - A_2\left(\cosh\left(\frac{MH}{h_0}\right) - 1\right) \\ &\quad \left. + \frac{{h_0}^3}{\mu M^3}\sinh\left(\frac{MH}{h_0}\right) - \frac{H{h_0}^2}{\mu M^2}A_3\right) \\ &\quad \times\left(\cosh\left(\frac{MH}{h_0}\right) + \frac{\alpha h_0}{\sqrt{k}M}\sinh\left(\frac{MH}{h_0}\right)\right)^{-1}, \\ A_1 &= \frac{2\alpha {h_0}^4}{\sqrt{k}\mu M^4}, \qquad A_2 = \frac{\alpha k {h_0}^2}{\sqrt{k}\mu D M^2}, \\ A_3 &= \cosh\left(\frac{MH}{h_0}\right) + \frac{\alpha h_0}{\sqrt{k}M}\sinh\left(\frac{MH}{h_0}\right). \end{aligned} \tag{16}$$

Substituting (14) in (15) and rearranging the terms, we get

$$\begin{aligned} &\frac{\partial}{\partial x}\left\{\left[F(H, M) - \frac{k\delta M^3}{1 + \phi M^2}\right]\frac{\partial p}{\partial x}\right\} \\ &\quad + \frac{\partial}{\partial y}\left\{\left[F(H, M) - \frac{k\delta M^3}{1 + \phi M^2}\right]\frac{\partial p}{\partial y}\right\} = -\mu M^3\frac{\partial H}{\partial t}. \end{aligned} \tag{17}$$

The above equation is the modified Reynolds equation that accounts the MHD and porous effects in the fluid film region. To study the effect of roughness, we take stochastic average of the Reynolds equation (17) as

$$\begin{aligned} &\frac{\partial}{\partial x}\left\{E\left[\left(F(H, M) - \frac{k\delta M^3}{1 + \phi\ M^2}\right)\frac{\partial p}{\partial x}\right]\right\} \\ &\quad + \frac{\partial}{\partial y}\left\{E\left[\left(F(H, M) - \frac{k\delta M^3}{1 + \phi M^2}\right)\frac{\partial p}{\partial y}\right]\right\} \\ &\quad = -\mu M^3\frac{\partial H}{\partial t}, \end{aligned} \tag{18}$$

where expectancy operator $E(\bullet)$ is defined by

$$E(\bullet) = \int_{-\infty}^{\infty}(\bullet)\ \ f(h_s)\, dh_s, \tag{19}$$

and $f(h_s)$ is the probability density function of the stochastic variable h_s. In many engineering applications, bearing surfaces show a roughness height distribution which is Gaussian in nature. Therefore, polynomial form which approximates the Gaussian is chosen in the analysis. Such a probability density function is given by Christensen [3] as

$$f(h_s) = \begin{cases} \frac{35}{32c^7}\left(c^2 - h_s^{\,2}\right)^3, & \text{if } -c < h_s < c; \\ 0, & \text{elsewhere,} \end{cases} \tag{20}$$

where c is the total range of random film thickness variable and function terminates at $c = \pm 3\sigma$, σ being the standard deviation.

There are two types of roughness patterns, namely, longitudinal and transverse roughness structures, given by the Christensen stochastic theory [3]. This stochastic theory helps us to derive the modified Reynolds equation for both longitudinal and transverse roughness structure. The longitudinal roughness structure has the form of narrow ridges and valleys across x directions, and the one-dimensional transverse structure where roughness striations run in the y directions in the form of narrows.

2.1. Longitudinal Roughness. In this case, as roughness has the form of narrow ridges running in the x-direction, film thickness takes the form

$$H = h_0 + h_s(x, \xi). \tag{21}$$

Then, (18) becomes

$$\begin{aligned} &\frac{\partial}{\partial x}\left\{\left(E(F(H,M)) - \frac{k\delta M^3}{1+\phi M^2}\right)\frac{\partial E(p)}{\partial x}\right\} \\ &\quad + \frac{\partial}{\partial y}\left\{\left(\frac{1}{E(1/F(H,M))} - \frac{k\delta M^3}{1+\phi M^2}\right)\frac{\partial E(p)}{\partial y}\right\} \\ &\quad = -\mu M^3 \frac{\partial E(H)}{\partial t}. \end{aligned} \tag{22}$$

2.2. Transverse Roughness. In this case, one-dimensional transverse roughness striations run in the y directions; hence, film thickness takes the form

$$H = h_0 + h_s(\gamma, \xi). \tag{23}$$

Then, (18) becomes

$$\begin{aligned} &\frac{\partial}{\partial x}\left\{\left(\frac{1}{E(1/F(H,M))} - \frac{k\delta M^3}{1+\phi M^2}\right)\frac{\partial E(p)}{\partial x}\right\} \\ &\quad + \frac{\partial}{\partial y}\left\{\left(E(F(H,M)) - \frac{k\delta M^3}{1+\phi M^2}\right)\frac{\partial E(p)}{\partial y}\right\} \\ &\quad = -\mu M^3 \frac{\partial E(H)}{\partial t}. \end{aligned} \tag{24}$$

However, we are focusing on one-dimensional longitudinal roughness since the transverse roughness structure can be obtained from the other by just rotation of coordinate axes. Therefore, the modified Reynolds equation (22) for one-dimensional longitudinal roughness is analysed for further investigation. In order to solve the modified Reynolds equation (22) for the pressure, the following boundary conditions are used

$$E(p) = 0, \quad \text{at } x = 0;\ a,\ y = 0;\ b, \tag{25}$$

where a and b are finite dimensions of plates in x and y directions, respectively.

From (19), we have

$$E(H) = h. \tag{26}$$

The following non-dimensional parameters and variables are introduced:

$$\begin{aligned} &\overline{x} = \frac{x}{a}, \quad \overline{y} = \frac{y}{b}, \quad \overline{H} = \frac{H}{h_0}, \quad \overline{p} = \frac{-h_0^{\,3} E(p)}{a^2 \mu (\partial h/\partial t)}, \\ &S = \frac{\alpha}{\sqrt{k}}, \quad S = \frac{\overline{S}}{h_0}, \quad \lambda = \frac{b}{a}, \quad \psi = \frac{k\delta}{h_0^{\,3}}, \end{aligned} \tag{27}$$

where C is the non-dimensional roughness parameter, p is the nondimensional fluid film pressure, λ is the aspect ratio, and S is the nondimensional slip velocity parameter; then (22), after dropping the overhead bars, becomes

$$\begin{aligned} &\frac{\partial}{\partial x}\left\{\left[E(F(H,M,S)) - \frac{M^3\psi}{1+\phi M^2}\right]\frac{\partial p}{\partial x}\right\} \\ &\quad + \frac{1}{\lambda^2}\frac{\partial}{\partial y}\left\{\left[\frac{1}{E(1/F(H,M,S))} - \frac{M^3\psi}{1+\phi M^2}\right]\frac{\partial p}{\partial y}\right\} \\ &\quad = M^3, \end{aligned} \tag{28}$$

where

$$\begin{aligned} &F(H,M,S) \\ &\quad = \left(-2S + \frac{\alpha^2 M^2}{S(1+\phi M^2)} + \right. \\ &\qquad \left(\left(-HM^2 + 2S - \frac{\alpha^2 M^2}{S(1+\phi M^2)}\right)\cosh(MH)\right. \\ &\qquad \left.\left. + \ (M - MHS)\sinh(MH)\right)\right) \\ &\qquad \times (M\cosh(MH) + S\sinh(MH))^{-1}, \end{aligned} \tag{29}$$

$$E(F(H,M,S)) = \frac{35}{32C^7}\int_{-C}^{C} F(H,M,S)\left(C^2 - h_s^2\right)^3 dh_s, \tag{30}$$

$$E(1/F(H,M,S)) = \frac{35}{32C^7}\int_{-C}^{C} \frac{\left(C^2 - h_s^2\right)^3}{F(H,M,S)} dh_s, \tag{31}$$

and boundary conditions (25) for the pressure field become

$$p = 0 \quad \text{at } x = 0;\ 1,\ y = 0;\ 1. \tag{32}$$

The above-modified Reynolds equation is too complicated to solve analytically, as there are two integral expressions (30) and (31) which are not solvable in closed form. Hence, we resort to solveing the modified Reynolds equation (28) by multigrid method.

3. Numerical Solution by Multigrid Method

The modified Reynolds equation (28) is elliptic in nature, which is very complicated to be solved analytically. Finite difference based multigrid method is used to solve this equation. This method provides us a simple way to compute pressure distribution. In multigrid method, few Gauss-Seidel iterations are applied for smoothing the errors. Half-weighting restriction operator is used for transferring the calculated residual to the coarser grid level. The procedure is repeated till the coarsest level is reached with just single unknown that can be solved exactly. Next, bilinear interpolation operator is used to prolongate the solution from coarsest level to next finer grid level and then apply few Gauss-Seidel iterations. Repeat this till the original level is reached. The number of grids in each direction is taken to be 257×257. Thus, there are 257×257 number of unknowns and hence equations in the problem. Convergent solution for the pressure is obtained when the pressure at two consecutive finest levels is almost the same: up to 10^{-6}. Simpson's 1/3rd rule is adopted to solve the expressions (30) and (31).

4. Results and Discussions

A simplified mathematical model has been developed to investigate the combined effects of roughness and magnetic field on squeeze film lubrication of two rectangular plates of which the upper plate has roughness and the lower plate has a porous material and discussed for various physical phenomena. Multigrid method solution to the Reynolds equation (28) has been obtained for the range for parameters $C = 0.1$–0.5, $M = 1$–10, and $\lambda = 0.1$–10 as these values are opted to be in the limit of parameters that have been used extensively in previous studies and experimental investigations. All the derived quantities such as pressure distribution and load capacity are obtained as a function of roughness (C), Hartmann number (M), permeability (ψ), and aspect ratio (λ) and are presented in Figures 2–6.

For $\psi \to 0$ (nonporous), $S \to \infty$ (no-slip), and $M \to 0$ (nonmagnetic), the present analysis, respectively reduces to the study of Bujurke and Kudenatti [12] wherein they study MHD lubrication between rough parallel plates, and the analysis of Lin [15] where the author studies MHD squeeze film characteristics for finite rectangular plates.

In Figures 2(a)–2(d), the deviation of pressure distribution with rectangular coordinates x and y for various parameters is represented. It is pragmatic that the effect of Hartmann number is to increase the pressure distribution in the fluid film region. For increasing M, the pressure distribution also increases (compare Figures 2(a) and 2(d)). Also note that for $M = 3$, $C = 0.2$, (Figure 2(b)) the consequence of roughness is to increase the pressure distribution compared to $C = 0.4$ (Figure 2(e)). The reason behind this is due to the application of magnetic field normal to the flow reducing the velocity of the lubricant in fluid film region. Thus, large amount of the fluid is retained in the film region, and this yields an increase in the pressure rise. Thus, velocity of the fluid reduces by the increase of application of magnetic field and consequently pressure rise increases. Furthermore, increase in the roughness increases the roughness asperities on bearing surface which further reduces the velocity of the fluid and also reduces the sidewise leakage of the fluid. Thus, pressure distribution also enhances.

4.1. Nondimensional Load Carrying Capacity. Load carrying capacity is one of the salient features of hydrodynamic characteristics of the bearing. This can be obtained once the fluid film pressure is calculated. The non-dimensional load carrying capacity W of the bearing surface per unit area in a non-dimensional form is

$$W = \iint_0^1 p(x, y)\, dx\, dy. \tag{33}$$

The variation of load carrying capacity W as a function of aspect ratio λ for different Hartmann number keeping other parameters constant is shown in Figure 3. The Hartmann number increases the load carrying capacity. The graph depicts that as M increases the load carrying capacity also increases. Furthermore, as aspect ratio λ increases from 0.1 to 10, the load carrying capacity also increases. As explained in the previous section, effects of roughness and Hartmann number are to reduce the velocity of the fluid; as a result pressure distribution increases in the fluid film region which yields an increase of the load capacity of the bearings.

The variation of load carrying capacity W as a function of aspect ratio λ for different values of roughness C keeping all other parameters constants is shown in Figure 4. It is interesting to note that there exists a critical value λ_c of the aspect ratio λ at which the effect of roughness vanishes. At the critical value λ_c ($\lambda_c = 1.5683$), for $\lambda > \lambda_c$, the effect of roughness increases the load carrying capacity, and for $\lambda < \lambda_c$, the trend reverses. This trend is observed in Figure 4. However, as aspect ratio λ increases from 0.1 to 10 load carrying capacity increases. Also as aspect ratio λ increases the load carrying capacity increases.

Figure 5 depicts the variation of load carrying capacity W as a function of permeability ψ keeping other parameters constant. The effect of Hartmann number is to increase the load carrying capacity for all parameters of M. Further, it is of interest to note that for increasing permeability (from 0.0001 to 1), the load carrying capacity decreases for all magnetic parameters M. The reason behind this is that as permeable surface becomes main path for the fluid to percolate into the porous, the fluid which is retained due to application of magnetic field decreases in the fluid film region. This decreases the pressure rise which results into decrease in the load carrying capacity. This trend can be seen in Figure 5.

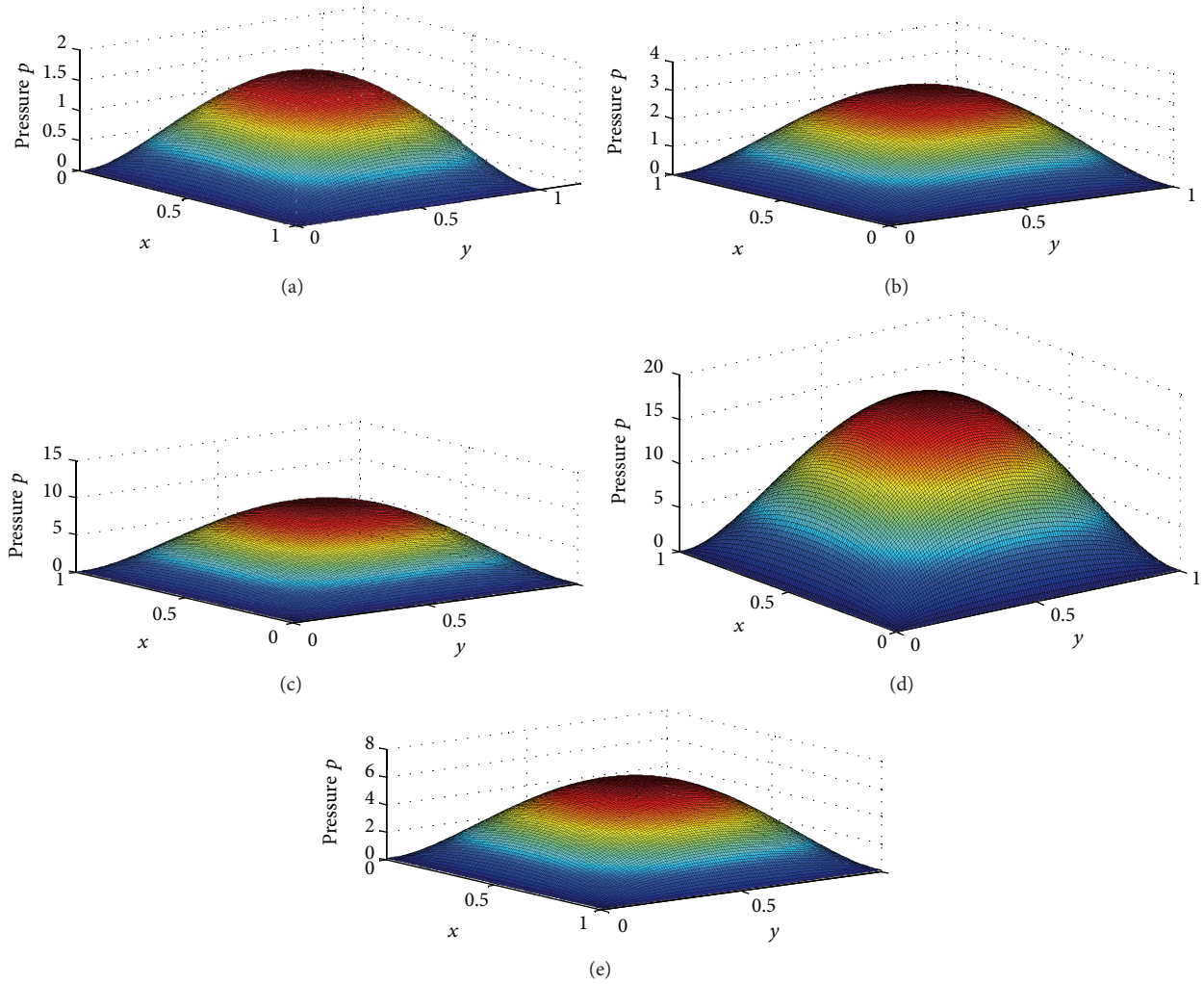

Figure 2: (a) Variation of distribution of pressure p for $C = 0.2$, $h = 0.5$, $\phi = 0.6$ and, $M = 1$. (b) Variation of distribution of pressure for $C = 0.2$, $h = 0.5$, $\phi = 0.6$, and $M = 3$. (c) Variation of distribution of pressure for $C = 0.2$, $h = 0.5$, $\phi = 0.6$, and $M = 7$. (d) Variation of distribution of pressure for $C = 0.2$, $h = 0.5$, $\phi = 0.6$, and $M = 10$. (e) Variation of distribution of pressure for $C = 0.4$, $h = 0.5$, $\phi = 0.6$, and $M = 3.0$.

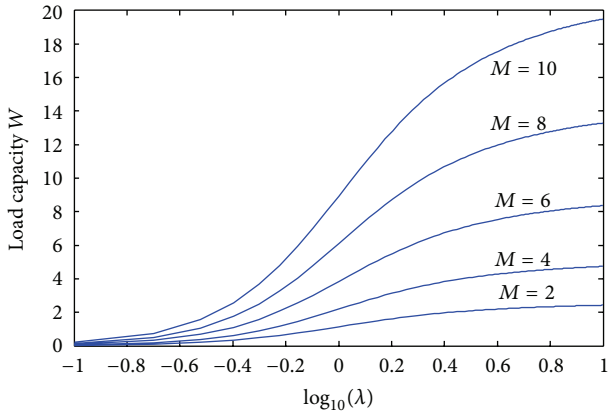

Figure 3: Variation of nondimensional load carrying capacity W with aspect ratio λ for $H = 0.5$, $\varphi = 0.6$, $\psi = 0.0001$.

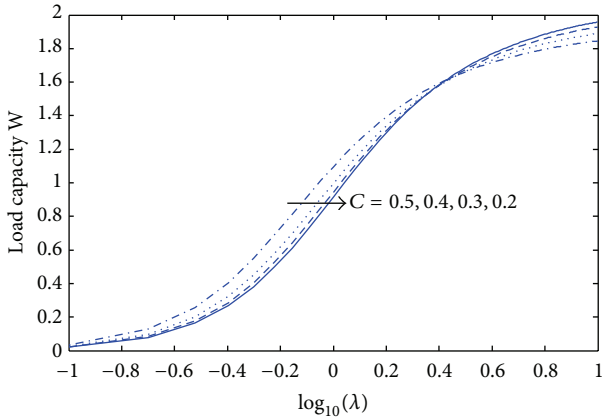

Figure 4: Variation of nondimensional load carrying capacity W with the aspect ratio λ for $H = 0.55$, $\psi = 0.0001$, and $M = 2$.

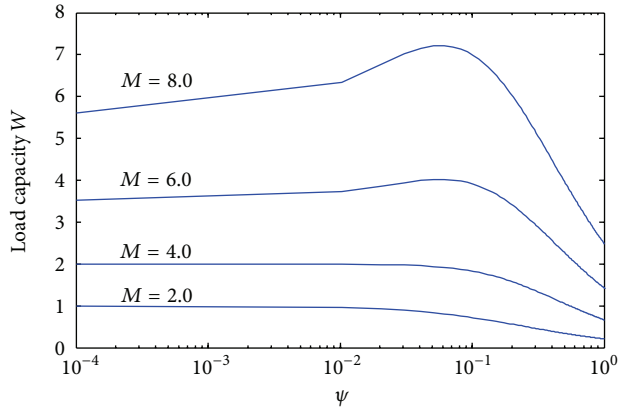

Figure 5: Variation of nondimensional load carrying capacity W as a function of permeability ψ for $C = 0.4$, $h = 0.5$, and $\lambda = 1$.

The similar trend has been observed in Figure 6 wherein we plot the load carrying capacity with the permeability ψ for different values of roughness parameter for C. Again, as roughness increases the load carrying capacity also increases, whereas for increasing ψ the load carrying capacity decreases.

5. Conclusions

The combined effects of roughness and magnetic field between two parallel plates of which the upper plate has rough surface and the lower plate has porous surface are studied using Christensen stochastic model for roughness.

Our investigations revealed the following.

(1) The pressure distribution and load carrying capacity increase for increasing roughness parameter (C).

(2) These bearing characteristics are found to increase for increasing Hartmann number (M).

(3) These characteristics decrease for increasing permeability parameter (ψ).

(4) Also, the load carrying capacity increases as the aspect ratio (λ) increases.

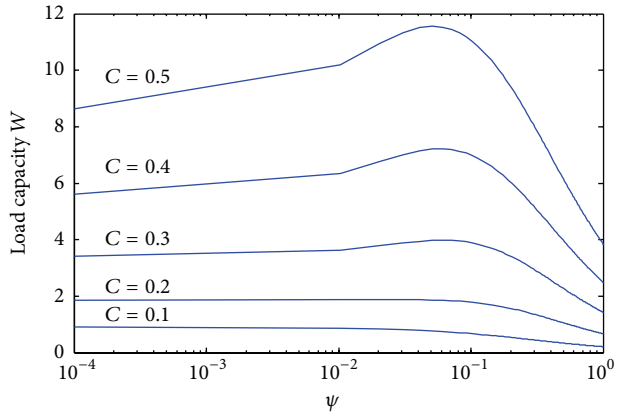

Figure 6: Variation of nondimensional load carrying capacity W as a function of permeability ψ for $M = 2$, $h = 0.5$, and $\lambda = 1$.

It is expected that these results help the lubrication engineers to choose the appropriate parameters for given magnetic field to enhance the life of the bearings.

Acknowledgment

The authors of the paper are thankful to the Principal management of JSS Academy of Technical Education, Bangalore, as well as M. S. Ramaiaha Institute of Technology, (Research Centre) Bangalore. The authors also thank anonymous reviewers for their valuable suggestions.

References

[1] M. G. Davies, "The generation of pressure between rough, fluid lubricated, moving, deformable surfaces," *Lubrication of Engineering*, vol. 19, p. 246, 1963.

[2] R. A. Burton, "Effect of two-dimensional sinusoidal roughness on the load support characteristics of a lubricant film," *Journal of Basic Engineering*, vol. 85, no. 2, p. 246, 1963.

[3] C. H. Christensen, "Stochastic models for hydrodynamic lubrication of rough surfaces," *Proceedings of the Institution of Mechanical Engineers*, vol. 184, no. 1, pp. 1013–1026, 1969.

[4] K. Gururajan and J. Prakash, "Roughness effects in a narrow porous journal bearing with arbitrary porous wall thickness," *International Journal of Mechanical Sciences*, vol. 44, no. 5, pp. 1003–1016, 2002.

[5] H. L. Chiang, C.-H. Hsu, and R. Lin, "Lubrication performance of finite journal bearings considering effects of couple stresses and surface roughness," *Tribology International*, vol. 37, no. 4, pp. 297–307, 2004.

[6] N. M. Bujurke and R. B. Kudenatti, "Surface roughness effects on squeeze film poroelastic bearings," *Applied Mathematics and Computation*, vol. 174, no. 2, pp. 1181–1195, 2006.

[7] S. Kamiyama, "Magnetohydrodynamic journal bearing (report 1)," *Journal of Lubrication Technology*, vol. 91, pp. 380–386, 1969.

[8] M. I. Anwar and C. M. Rodkiewicz, "Nonuniform magnetic field effects in MHD slider bearing," *Journal of Lubrication Technology*, vol. 94, no. 1, pp. 101–105, 1972.

[9] E. A. Hamza, "Magnetohydrodynamic effects on a fluid film squeezed between two rotating surfaces," *Journal of Physics D*, vol. 24, no. 4, pp. 547–554, 1991.

[10] E. R. Maki, D. C. Kuzma, and R. L. Donnelly, "Magnetohydrodynamic lubrication flow between parallel plates," *Journal of Fluid Mechanics*, vol. 26, pp. 537–543, 1966.

[11] J. B. Shukla, "Hydromagnetic theory of squeeze films," *Journal of Basic Engineering*, vol. 87, pp. 142–144, 1965.

[12] N. M. Bujurke and R. B. Kudenatti, "MHD lubrication flow between rough rectangular plates," *Fluid Dynamics Research*, vol. 39, no. 4, pp. 334–345, 2007.

[13] G. S. Beavers and D. D. Joseph, "Boundary conditions at a naturally permeable wall," *Journal of Fluid Mechanics*, vol. 30, no. 1, pp. 197–207, 1967.

[14] V. T. Morgan and A. Cameron, "The mechanism of lubrication on porous metal bearings," in *Proceedings of the Conference on Lubrication and Wear*, vol. 89, pp. 151–157, Institute of Mechanical Experiments, London, UK, 1957.

[15] J. R. Lin, "Magneto-hydrodynamic squeeze film characteristics for finite rectangular plates," *Industrial Lubrication and Tribology*, vol. 55, no. 2, pp. 84–89, 2003.